

# Recursive Attitude Determination from Vector Observations: Euler Angle Estimation

I.Y. Bar-Itzhack\* and M. Idan†

*Technion—Israel Institute of Technology, Haifa, Israel*

This work presents an algorithm that processes a sequence of pairs of measured vectors to obtain a minimum variance estimate of the Euler angles which describe the attitude between two coordinate systems. The measurement equation is nonlinear and, unlike the direction cosine matrix and the quaternion estimation problems, the dynamics of the estimated angles are nonlinear as well. The algorithm can also handle singular cases, thus extending the use of Euler angles to all-attitude vehicles. Results of Monte-Carlo simulations are presented that demonstrate the efficiency of the algorithm. This work is a natural extension of the algorithms that were recently developed for estimating the direction cosine matrix and the quaternion, therefore it completes the set of recursive minimum variance algorithms for estimating the three common forms of expressing attitude.

## I. Introduction

ATTITUDE determination is an important element in guidance and control of flight vehicles. The three basic representations of attitude are Euler angles, direction cosine matrices (DCM), and quaternions. These representations express the orientation of a coordinate system fixed in the body (body system) with respect to some reference coordinate system (reference system). There are cases in which the orientation has to be extracted from the measurement of vectors in the two coordinate systems. That is, a sequence of vectors is measured both in the body and in the reference systems and the attitude has to be computed from the measured data. Typical cases where this problem arises are space missions such as the Small Astronomy Satellite, Seasat, Atmospheric Explorer Missions, and Magsat.<sup>1</sup> Another example is the Solar Maximum Mission spacecraft that used two fixed-head star trackers and a fine pointing sun sensor to measure vectors in body coordinates.<sup>2</sup> The same vectors can be computed in orbit-fixed coordinates using position information. The latter can be viewed as measurements in the reference (orbit-fixed) coordinate system.

In the past, attention was given to the direct computation of either the DCM or the quaternion from vector measurements but not to that of the Euler angles. A purely deterministic approach to the DCM computation was considered by Lerner<sup>3</sup> and Shuster and Oh.<sup>1</sup> Batch least square fitting<sup>4,5</sup> and recursive least squares filtering<sup>6</sup> were also applied to the computation of the DCM. The latest natural extension to this work was a derivation of a recursive minimum variance algorithm<sup>7</sup> which used a Kalman filter and an identification method to compute the DCM. Few researchers selected the quaternion to determine the attitude from vector measurements. Batch weighted least square fitting<sup>1,8</sup> and recursive methods<sup>9-11</sup> were used to compute the quaternion.

Until now, very little attention was given to the computation of the Euler angles directly from vector measurements and in cases where this was done,<sup>12,13</sup> the solution was an ad

hoc solution to satellite attitude determination which included satellite dynamics. The reason for that is, perhaps, the fact that the use of Euler angles for attitude tracking is hampered by possible singularities. In many cases, though, the vehicle is not an all-attitude vehicle (e.g., passenger and cargo planes, helicopters, roll stabilized missile, etc.) Consequently, no singularity is encountered when using Euler angles to compute the attitude from rate measurements. A typical example is a roll-stabilized sea-launched missile whose attitude is computed continuously during the mission using rate measurements to solve the Euler angle differential equations. The use of Euler angles is advantageous since the steering commands are explicit functions of the vehicle Euler angles. During the initial alignment phase, the angular velocity vector of the missile is measured in body coordinates by the missile's own gyros. The same angular velocity vector is also measured by other gyros in the ship-fixed coordinate system. The initial Euler angles have to be computed, then, from vector measurements in two different coordinate systems. Although Euler angles are used only in attitude-limited vehicles, no singularity is encountered even in all-attitude vehicles in the instantaneous determination of the attitude, even when Euler angle representation is used to express the orientation. Singularity arises only in the solution of the differential equations which describe the time history of the Euler angles. Therefore, depending on the required accuracy and availability of vector observations, Euler angles may be used in certain cases even in all-attitude vehicles. This point will be demonstrated later.

It should be noted that, typically, when dealing with attitude determination from vector observations, two algorithms are involved. The first algorithm is a numerical solution of the differential equations that describe the rate of change of the attitude parameters (e.g., direction cosines, quaternion, Euler angles). The second algorithm is the estimator that yields an instantaneous estimate of the attitude parameters based on external measurements which, in the present case, are vectors measured in two coordinate systems. The decision as to which parameters are to be used in the second algorithm—that is, the decision whether to estimate the direction cosines, quaternion, or the Euler angles which describe the attitude of the vehicle—is not uncoupled from the first algorithm. In fact, the choice of the attitude parameters of the first algorithm practically dictates the parameters to be estimated. This stems from the fact that the estimator needs to compute certain matrices whose entries are computed by the first algorithm for its own use. Thus, if Euler angles are used continuously to compute the

Presented as Paper 85-1959 at the AIAA Guidance, Navigation, and Control Conference, Snowmass, CO, Aug. 19-21, 1985; received Jan. 29, 1986; revision received June 2, 1986. Copyright © 1986 by I.Y. Bar-Itzhack. Published by the American Institute of Aeronautics and Astronautics, Inc., with permission.

\*Professor, Department of Aeronautical Engineering.

†Graduate Student, Department of Aeronautical Engineering.

attitude of the vehicle from gyro measurements, it is very inefficient to use parameters other than Euler angles in the estimator.

In the present work we develop an extended Kalman filter algorithm for determining the attitude by Euler angles directly from vector measurements. It is a natural extension of the work reported in Refs. 7 and 10 and completes the set of recursive minimum variance algorithms for computing the corresponding three common forms of expressing attitude. This, in fact, is the main purpose of the present work; however, in view of the foregoing discussion, the results of this work certainly have a practical merit too.

The problem that is treated in this work is presented in Sec. II. A modified version of the extended Kalman filter for solving the problem is developed in Sec. III. Section IV presents results of Monte-Carlo simulation runs for static and dynamic cases as well as for a nearly singular case. The conclusions drawn from this work are summarized in Sec. V.

## II. Problem Statement

Let  $v$  denote the body fixed coordinate system and let  $u$  denote the reference system. Let  $\alpha$  denote the three Euler angles  $\psi$ ,  $\theta$ , and  $\phi$ , assembled into one column matrix; that is,

$$\alpha^T = [\psi, \theta, \phi] \quad (1)$$

where  $T$  denotes the transpose. These Euler angles describe the attitude of the body with respect to the reference coordinate system where the order of rotation is chosen to be  $z$ ,  $y$ , and  $x$ . Let  $D$  denote the DCM that transforms vectors from  $u$  to  $v$ . Obviously,  $D$  is a function of  $\alpha$ , denoted by  $D(\alpha)$ . A sequence of vectors  $\bar{r}_i$ ,  $i = 1, 2, \dots, N$  is measured both in  $u$  and in  $v$ . The measurements in system  $u$  result in the sequence  $u_i$ ,  $i = 1, 2, \dots, N$  of column matrices; whereas in system  $v$ , the measurements result in the corresponding sequence  $v_i$ ,  $i = 1, 2, \dots, N$ . The column matrices  $u_i$  and  $v_i \in R^3$ . We wish to compute  $\hat{\alpha}$ , the minimum variance estimate of  $\alpha$ .

## III. Problem Solution

We use a recursive estimation process to estimate  $\alpha$ . Let  $v_{o,i}$ ,  $u_{o,i}$  and  $D(\alpha_i)$  denote the correct values of  $v_i$ ,  $u_i$ , and the DCM, respectively, at this instant. Certainly

$$v_{o,i+1} = D(\alpha_{i+1}) u_{o,i+1} \quad (2)$$

The measurements  $u_{i+1}$  and  $v_{i+1}$  can be written as

$$u_{i+1} = u_{o,i+1} + n_{u,i+1} \quad (3)$$

$$v_{i+1} = v_{o,i+1} + n_{v,i+1} \quad (4)$$

where  $n_u$  and  $n_v$  are the zero mean measurement noise vectors, which, for simplicity, are assumed to be white, and their respective covariance matrices  $R_{u,i+1}$  and  $R_{v,i+1}$  are known. When  $n$  are not white but can be expressed as an output of a linear system driven by white noise, the problem can still be handled using standard techniques.<sup>14,15</sup> (We purposely do not assume a particular set of measuring devices in order not to limit the scope of this work. The general treatment presented here can, of course, be adopted to a particular system using those standard techniques.) Let us express  $\alpha_{i+1}$  as

$$\alpha_{i+1} = \hat{\alpha}_{i+1/i} + \delta\alpha_{i+1} \quad (5)$$

that is,  $\alpha_{i+1}$  is expressed as the sum of our estimate of  $\alpha$  at the  $(i+1)$ st stage based on past measurements (up to and including the  $i$ th measurement) and a difference  $\delta\alpha_{i+1}$  between the true value of  $\alpha$  and its estimate. At this stage we wish to

use the  $(i+1)$ st measurement given by Eqs. (3) and (4) to estimate  $\delta\alpha$  and add the estimate to  $\hat{\alpha}_{i+1/i}$  to obtain the updated estimate of  $\alpha$ , which we denote by  $\hat{\alpha}_{i+1/i+1}$ . To meet this end, substitute Eqs. (3-5) into Eq. (2) to obtain

$$v_{i+1} = D(\hat{\alpha}_{i+1/i} + \delta\alpha_{i+1}) (u_{i+1} - n_{u,i+1}) + n_{v,i+1} \quad (6)$$

Next, expand  $D(\hat{\alpha}_{i+1/i} + \delta\alpha_{i+1})$  about  $\hat{\alpha}_{i+1/i}$ , retaining only the linear terms in  $\delta\alpha_{i+1}$ , and substitute the result into Eq. (6). To accomplish this, let us write the explicit functional relationship between the DCM and the Euler angles

$$D(\alpha) = \begin{bmatrix} c\psi \cdot c\theta & s\psi \cdot c\theta & -s\theta \\ c\psi \cdot s\theta \cdot s\phi & s\psi \cdot s\theta \cdot s\phi & c\theta \cdot s\phi \\ -s\psi \cdot c\phi & +c\psi \cdot c\phi & \\ c\psi \cdot s\theta \cdot c\phi & s\psi \cdot s\theta \cdot c\phi & c\theta \cdot c\phi \\ +s\psi \cdot s\phi & -c\psi \cdot s\phi & \end{bmatrix} \quad (7)$$

where  $c$  and  $s$  denote the cosine and sine functions, respectively. Now,

$$D(\hat{\alpha}_{i+1/i} + \delta\alpha_{i+1}) \sim D(\hat{\alpha}_{i+1/i}) + \left. \frac{\partial D}{\partial \psi} \right|_{\hat{\alpha}_{i+1/i}} \delta\psi_{i+1} + \left. \frac{\partial D}{\partial \theta} \right|_{\hat{\alpha}_{i+1/i}} \delta\theta_{i+1} + \left. \frac{\partial D}{\partial \phi} \right|_{\hat{\alpha}_{i+1/i}} \delta\phi_{i+1} \quad (8)$$

Using Eq. (7), we obtain the three derivatives of  $D$  with respect to the Euler angles as follows:

$$A_1 \triangleq \left. \frac{\partial D}{\partial \psi} \right|_{\hat{\alpha}_{i+1/i}} = \begin{bmatrix} -s\psi \cdot c\theta & c\psi \cdot c\theta & 0 \\ -s\psi \cdot s\theta \cdot s\phi & c\psi \cdot s\theta \cdot s\phi & 0 \\ -c\psi \cdot c\phi & -s\psi \cdot c\phi & \\ -s\psi \cdot s\theta \cdot c\phi & c\psi \cdot s\theta \cdot c\phi & 0 \\ +c\psi \cdot s\phi & +s\psi \cdot s\phi & \end{bmatrix}_{\hat{\alpha}_{i+1/i}} \quad (9a)$$

$$A_2 \triangleq \left. \frac{\partial D}{\partial \theta} \right|_{\hat{\alpha}_{i+1/i}} = \begin{bmatrix} -c\psi \cdot s\theta & -s\psi \cdot s\theta & -c\theta \\ c\psi \cdot c\theta \cdot s\phi & s\psi \cdot c\theta \cdot s\phi & -s\theta \cdot s\phi \\ c\psi \cdot c\theta \cdot c\phi & s\psi \cdot c\theta \cdot c\phi & -s\theta \cdot c\phi \end{bmatrix}_{\hat{\alpha}_{i+1/i}} \quad (9b)$$

$$A_3 \triangleq \left. \frac{\partial D}{\partial \phi} \right|_{\hat{\alpha}_{i+1/i}} = \begin{bmatrix} 0 & 0 & 0 \\ c\psi \cdot s\theta \cdot c\phi & s\psi \cdot s\theta \cdot c\phi & c\theta \cdot c\phi \\ +s\psi \cdot s\phi & -c\psi \cdot s\phi & \\ -c\psi \cdot s\theta \cdot s\phi & -s\psi \cdot s\theta \cdot s\phi & -c\theta \cdot s\phi \\ -s\psi \cdot c\phi & -c\psi \cdot c\phi & \end{bmatrix}_{\hat{\alpha}_{i+1/i}} \quad (9c)$$

With the above definition of  $A_j$ ,  $j = 1, 2, 3$ , we can write Eq. (8) as

$$D(\hat{\alpha}_{i+1/i} + \delta\alpha) \sim D(\hat{\alpha}_{i+1/i}) + \sum_{j=1}^3 A_j \cdot \delta\alpha_{j,i+1} \quad (10)$$

which, when substituted into Eq. (6), yields

$$v_{i+1} = \left[ D(\hat{\alpha}_{i+1/i}) + \sum_{j=1}^3 A_j \cdot \delta\alpha_{j,i+1} \right] (u_{i+1} - n_{u,i+1}) + n_{v,i+1}$$

Neglecting the products of  $\delta\alpha_j$  and  $n_{u,i+1}$ , which are both small, we obtain

$$v_{i+1} - D(\hat{\alpha}_{i+1/i})u_{i+1} = \sum_{j=1}^3 A_j u_{i+1} \cdot \delta\alpha_{j,i+1} - D(\hat{\alpha}_{i+1/i})n_{u,i+1} + n_{v,i+1} \quad (11)$$

Define the observation matrix  $H_{i+1/i}$  by its columns as follows:

$$H_{i+1/i} = [h_1, h_2, h_3] \quad (12a)$$

where

$$h_j \triangleq A_j u_{i+1} \quad j=1,2,3 \quad (12b)$$

Also, define the following noise vector

$$n_{i+1} \triangleq n_{v,i+1} - D(\hat{\alpha}_{i+1/i})n_{u,i+1} \quad (12c)$$

and the observation vector

$$e_{i+1} \triangleq v_{i+1} - D(\hat{\alpha}_{i+1/i})u_{i+1} \quad (12d)$$

then Eq. (11) can be written as

$$e_{i+1} = H_{i+1/i}\delta\alpha_{i+1} + n_{i+1} \quad (13)$$

Note that  $n_{i+1}$ , defined in Eq. (12c), is a zero mean white noise vector whose covariance matrix  $R_{i+1}$  can be computed as follows:

$$R_{i+1/i} = R_{v,i+1} + D(\hat{\alpha}_{i+1/i})R_{u,i+1}D(\hat{\alpha}_{i+1/i})^T \quad (14)$$

Now  $e_{i+1}$  is data which we obtain when we process the measurements  $u_{i+1}$  and  $v_{i+1}$ , using Eqs. (7) and (12d). Since  $n_{i+1}$  is zero mean white noise with known covariance, the linear relationship between  $e_{i+1}$  and  $\delta\alpha$ , expressed in Eq. (13), enables us to estimate the difference  $\delta\alpha$  between  $\hat{\alpha}_{i+1/i}$ , our current estimate of  $\alpha$ , and its true value. We distinguish between two cases, a static one and a dynamic one.

#### Static Case

When the vehicle is not rotating with respect to the reference system,  $\alpha$  is constant and by successive measurements and estimation we can have  $\alpha_i$  approach  $\alpha$  using the following algorithm:

##### Between Measurements

$$\hat{\alpha}_{i+1/i} = \hat{\alpha}_{i/i} \quad (15a)$$

$$P_{i+1/i} = P_{i/i} \quad (15b)$$

##### Across Measurements

$$K_{i+1} = P_{i+1/i}H_{i+1/i}^T [H_{i+1/i}P_{i+1/i}H_{i+1/i}^T + R_{i+1/i}]^{-1} \quad (15c)$$

$$\delta\hat{\alpha}_{i+1/i+1} = K_{i+1}e_{i+1} \quad (15d)$$

$$\hat{\alpha}_{i+1/i+1} = \hat{\alpha}_{i+1/i} + \delta\hat{\alpha}_{i+1/i+1} \quad (15e)$$

$$P_{i+1/i+1} = (I - K_{i+1}H_{i+1/i+1})P_{i+1/i}(I - K_{i+1}H_{i+1/i+1})^T + K_{i+1}R_{i+1/i+1}K_{i+1}^T \quad (15f)$$

Note that here, unlike in the ordinary extended Kalman filter, before computing  $P_{i+1/i+1}$ ,  $H$  and  $R$  are recomputed using the

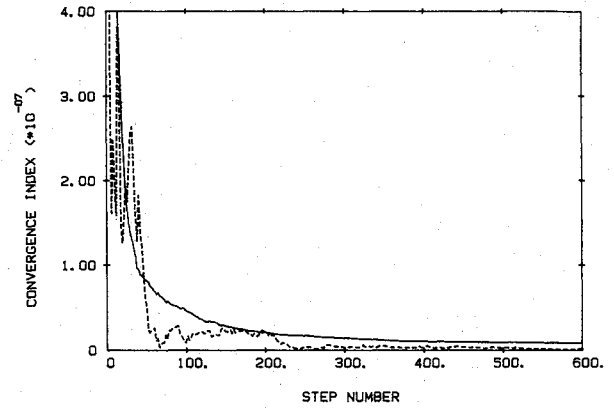


Fig. 1 Behavior of the convergence index in the static case. The broken line shows  $J_{i+1}(1)$  and the solid line shows  $J_{i+1}$ .

latest estimate of  $\alpha$ . It was empirically found that this yields a faster converging algorithm.

#### Dynamic Case

When the orientation is changing and we measure the angular rate at which the body coordinates rotate with respect to the reference system, we can solve the following differential equations to obtain  $\alpha$ , provided the initial value of  $\alpha$  is known and  $\omega$ , the angular rate vector, is measured precisely.

$$\dot{\psi} = \frac{1}{\cos\theta} (\omega_y \sin\phi + \omega_z \cos\phi) \quad (16a)$$

$$\dot{\theta} = \omega_y \cos\phi - \omega_z \sin\phi \quad (16b)$$

$$\dot{\phi} = \omega_x + \tan\theta (\omega_y \sin\phi + \omega_z \cos\phi) \quad (16c)$$

where  $\omega_x$ ,  $\omega_y$ , and  $\omega_z$  denote the three components of  $\omega$  when resolved in the body axes. Since we do not know the initial value of  $\alpha$  precisely, and  $\omega$  is not measured perfectly, Eqs. (16) do not yield the correct value of  $\alpha$ . However, we can use the vector observations in order to estimate  $\alpha$ . Another way of looking at it is to consider the dynamic case as an extension of the static case in the sense that the knowledge of the dynamics of  $\alpha$ , which are given in Eqs. (16), enables us to relate past estimates of  $\alpha$  to the present estimate and thereby utilize past measurements to obtain a better estimate at the present stage, rather than obtain an estimate which is based only on the present measurement.

The problem of estimating the direction cosine matrix and the quaternion from vector observations, which was solved in the past,<sup>7,10,11</sup> dealt with a nonlinear relationship between the observed and the estimated quantities, but, on the other hand, the dynamics were linear. Here, the measurement, as well as the dynamics equations, is nonlinear, as can be seen in Eqs. (6), (7), and (16). The dynamics equations can be expressed in the following general form:

$$\dot{\alpha} = f(\alpha, \omega) \quad (17)$$

In correspondence with the discrete expression given in Eq. (5), we can write the following continuous relationship between  $\alpha$ ,  $\hat{\alpha}$ , and  $\delta\hat{\alpha}$ :

$$\alpha = \hat{\alpha} + \delta\alpha \quad (18)$$

Also note that  $\omega$  is not measured precisely; thus we actually obtain an approximate value  $\tilde{\omega}$ , which is related to  $\omega$  through

$$\tilde{\omega} = \omega + \delta\omega \quad (19)$$

where  $\delta\omega$  is the measurement noise of  $\omega$ . For simplicity, this noise is assumed to be zero mean and white, where

$$E\{\delta\omega(t)\delta\omega(t-\tau)^T\} = Q\delta(t-\tau) \quad (20)$$

and  $Q$  is known. We use this simple model in order to focus the attention on the estimation algorithm of the Euler angles themselves with the knowledge that the inclusion of typical gyro models is straightforward (see Ref. 15, pp. 78-84) and well known. Using Eqs. (18) and (19), Eq. (17) can be written as

$$\dot{\hat{\alpha}} + \delta\dot{\alpha} = f(\hat{\alpha} + \delta\alpha, \tilde{\omega} - \delta\omega) \quad (21)$$

In our algorithm we shall propagate  $\hat{\alpha}$  in time according to the differential equation

$$\dot{\hat{\alpha}} = f(\hat{\alpha}, \tilde{\omega}) \quad (22)$$

Therefore, in the following development of Eq. (21) into a first order Taylor series,

$$\dot{\hat{\alpha}} + \delta\dot{\alpha} \sim f(\hat{\alpha}, \tilde{\omega}) + \left. \frac{\partial f}{\partial \alpha} \right|_{\hat{\alpha}, \tilde{\omega}} \delta\alpha - \left. \frac{\partial f}{\partial \omega} \right|_{\hat{\alpha}, \tilde{\omega}} \delta\omega \quad (23)$$

the first terms on both sides balance each other such that

$$\delta\dot{\alpha} \sim \left. \frac{\partial f}{\partial \alpha} \right|_{\hat{\alpha}, \tilde{\omega}} \delta\alpha - \left. \frac{\partial f}{\partial \omega} \right|_{\hat{\alpha}, \tilde{\omega}} \delta\omega \quad (24)$$

Define the matrices  $F$  and  $G$  as follows:

$$F = \left. \frac{\partial f}{\partial \alpha} \right|_{\hat{\alpha}, \tilde{\omega}} \quad (25a)$$

$$G = - \left. \frac{\partial f}{\partial \omega} \right|_{\hat{\alpha}, \tilde{\omega}} \quad (25b)$$

then Eq. (24) can be written as

$$\delta\dot{\alpha} \sim F\delta\alpha + G\delta\omega \quad (26)$$

where, from Eqs. (16) and (25),

$$F = \begin{bmatrix} 0 & \frac{t\theta}{c\theta}(\omega_y \cdot s\phi + \omega_z \cdot c\phi) & \frac{1}{c\theta}(\omega_y \cdot c\phi - \omega_z \cdot s\phi) \\ 0 & 0 & -(\omega_y \cdot s\phi + \omega_z \cdot c\phi) \\ 0 & \frac{1}{c^2\theta}(\omega_y \cdot s\phi + \omega_z \cdot c\phi) & t\theta(\omega_y \cdot c\phi - \omega_z \cdot s\phi) \end{bmatrix}_{\hat{\alpha}, \tilde{\omega}} \quad (27a)$$

$$G = \begin{bmatrix} 0 & -\frac{s\phi}{c\theta} & -\frac{c\phi}{c\theta} \\ 0 & -c\phi & s\phi \\ -1 & -t\theta \cdot s\phi & -t\theta \cdot c\phi \end{bmatrix}_{\hat{\alpha}} \quad (27b)$$

and where  $t$  denotes the tangent function. Having expressed the dynamics of  $\delta\alpha$  in a linear form, where  $F$  and  $G$  are computable, the algorithm for the dynamic case follows immediately. In fact, only two changes have to be made in the algorithm of the static case given in Eq. (15) to be able to accommodate the dynamic case as well; namely, the algorithm

for propagating  $\hat{\alpha}$  and  $P$  between measurements [Eqs. (15a) and (15b)] has to be changed into

$$\dot{\hat{\alpha}}(t) = f[\hat{\alpha}(t), \tilde{\omega}(t)] \quad (28a)$$

$$P(t) = F[\hat{\alpha}(t), \tilde{\omega}(t)]P(t) + P(t)F[\hat{\alpha}(t), \tilde{\omega}(t)]^T + G[\hat{\alpha}(t)]QG[\hat{\alpha}(t)]^T \quad (28b)$$

The last two differential equations have to be solved from time  $t_i$  to  $t_{i+1}$ , starting with the initial conditions  $\hat{\alpha}(t_i) = \hat{\alpha}_{i/i}$  and  $P(t_i) = P_{i/i}$ . The values of  $\hat{\alpha}$  and  $P$  at  $t_{i+1}$  are denoted by  $\hat{\alpha}_{i+1/i}$  and  $P_{i+1/i}$ , respectively.

Equation (28b) can be solved in a discrete form as follows:

$$P_{i+1/i} = \Phi_i P_{i/i} \Phi_i^T + G_i Q_i G_i^T \quad (29)$$

where  $\Phi_i$  is the transition matrix of  $F$ , and  $G_i Q_i G_i^T$  is obtained from the discretization of the  $GQG^T$  matrix.<sup>15</sup> The latter is not that simple to compute; however, an exact value for  $G_i Q_i G_i^T$  is not required since, even when great care is taken in computing this term, tuning is usually needed to obtain the best convergence characteristics of the filter,<sup>16</sup> and tuning requires an empirical adjustment of this matrix (see Sec. IV).

#### IV. Monte-Carlo Simulations

In order to evaluate the performance of the estimator, we define a *convergence index* as follows:

$$J_{i+1} = \text{trace}[(D_{i+1} - \hat{D}_{i+1/i+1})^T (D_{i+1} - \hat{D}_{i+1/i+1})] \quad (30)$$

where  $\hat{D}_{i+1/i+1} = D(\hat{\alpha}_{i+1/i+1})$ , and  $D_{i+1} = D(t_{i+1})$ . Since the estimate  $\hat{\alpha}_{i+1/i+1}$  is a random variable, one sample run does not adequately express the results. Therefore, we calculate and present a sample average of  $J_{i+1}$  over 100 runs. The sample average  $\bar{J}_{i+1}$  is defined and evaluated as follows:

$$\bar{J}_{i+1} \triangleq E\{J_{i+1}\} \sim \frac{1}{100} \sum_{k=1}^{100} J_{i+1}(k) \quad (31)$$

Three cases of Monte-Carlo simulations were run: a static case, a dynamic case, and a singular case. All three cases started with the same initial orientation defined by  $\alpha_0^T = [10, 20, \text{ and } 30 \text{ deg}]$ ; however, the initial estimate  $\hat{\alpha}_0$  was zero in all cases. This large difference between the actual Euler angles and their corresponding estimates was chosen in order to demonstrate the robustness of the algorithm to large initial estimation errors. The standard deviation of all the components of the measurement noise  $n_u$  and  $n_v$  corresponded to an angular error of 100 arc sec. Figure 1 presents simulation results for the static case. The broken line shows the time

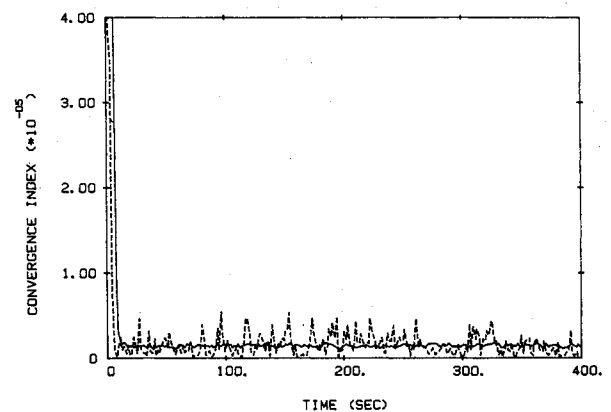


Fig. 2 Behavior of the convergence index in the dynamic case with tuning. The broken line shows  $J_{i+1}(1)$  and the solid line shows  $\bar{J}$ .

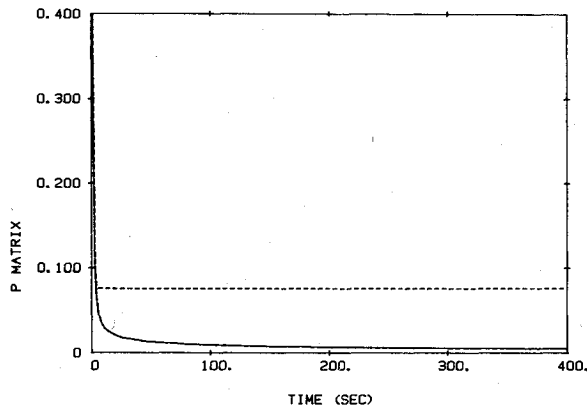


Fig. 3 Covariance change as a result of tuning. The solid line shows the root of the trace of the  $P$  matrix before tuning and the broken line shows it after tuning.

behavior of the convergence index  $J_{i+1}(1)$  for the first sample run, and the solid line shows the behavior of  $\bar{J}_{i+1}$ , the averaged convergence index. The dynamic case was run with the angular velocity vector  $\omega^T = [10., 2., 2.]$  deg/s. We assume that the gyros that measure  $\omega$  produce an additive error, which is characterized as white noise whose spectral density is 0.01 deg/h<sup>3/2</sup> for each gyro. The time interval between time updates was 0.05 s, and the time between measurements was 1 s. The results of this run are shown in Fig. 2, where, again, the broken line shows the convergence index  $J_{i+1}(1)$  and the solid line shows  $\bar{J}_{i+1}$ . In this estimator, tuning was required since  $\bar{J}_{i+1}$  reached a minimum and then started a slow divergence without tuning. This phenomenon is well known. It occurs when the filter model does not exactly match the real model and, in particular, when the driving noise of the real dynamics model is larger than that used in the filter. Consequently, the covariance matrix computed by the filter decreases to levels which are too low. This, in turn, produced too low filter gains and thus the filter rejects new measurements which are necessary to check the divergence of the estimation errors. The tuning action that eliminated this divergence was accomplished by bounding the lower values of the diagonal elements of the a priori covariance matrix  $P_{i+1/i}$ . This was achieved by increasing the main diagonal elements of  $G_i Q_i G_i^T$  [see Eq. (29)] whenever the corresponding elements of  $P_{i+1/i}$  decreased below their lower bounds. The lower bounds of  $P_{i+1/i}$  were selected to be the corresponding values of the main diagonal elements of  $P_{i+1/i}$  7 s from the beginning of the estimation process. These values were chosen because of the sharp convergence of the estimation errors at that time.

Figure 3 shows the amount of tuning necessary to achieve the stability demonstrated in Fig. 2. The solid line shows the square root of the sum of the main diagonal of  $P$  before tuning, and the broken line shows that value after tuning. Finally, several singular cases were also run. To obtain a singular case, the angular velocity vector was chosen to be  $\omega^T = [5., 5., 5.]$  deg/s. In this case singularity occurs whenever  $\theta$  reaches 90 deg, since then  $\cos\theta = 0$ . (Note that singularity occurs when all three components of  $\omega$  are equal and enough time elapses for the singularity to occur.) This blows up  $\psi$  and  $\phi$  in Eqs. (16), which describe the dynamics of  $\alpha$  and  $\dot{\alpha}$ . In addition, as can be seen in Eq. (27),  $F$  and  $G$  blow up too. This singularity can be overcome by freezing  $1/\cos\theta$  and  $1/\cos\dot{\theta}$  at the highest acceptable value determined by the processor. This will slightly change the nonlinear and linearized dynamics equations; however, the updates of  $\hat{\alpha}$ , which are based on the vector measurement, will maintain the accuracy of the estimate, which may be slightly degraded for a while but will still meet the required accuracy. Figure 4 shows the results of this run in terms of  $J_{i+1}(1)$  and  $\bar{J}_{i+1}$ . The highest value  $1/\cos\theta$  took in these runs was about 100. Note that at the singularity there is an ambiguity in  $\psi$  and  $\phi$ . The ambiguity means that  $\hat{\psi}$  and  $\hat{\phi}$

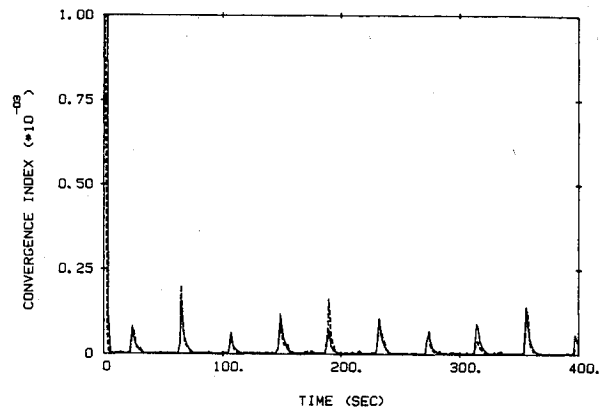


Fig. 4 Behavior of the convergence index in the singular case. The broken line shows  $J_{i+1}(1)$  and the solid line shows  $\bar{J}_{i+1}$ . The peaks occur at the singularities.

describe, together with  $\hat{\theta}$ , the correct orientation, although  $\hat{\psi}$  and  $\hat{\phi}$  are not respectively equal to  $\psi$  and  $\phi$ .

Finally, note that while the DCM has to satisfy the orthogonality condition and the quaternion has to satisfy the normality condition, Euler angles are not restricted by a similar constraint. Therefore, while the orthogonality property of the DCM was used to improve the convergence of the algorithm for estimating the DCM directly from vector measurements<sup>7</sup> and the normality property was used to improve the estimation of the quaternion,<sup>10</sup> no such property can be used here to speed up the convergence of the Euler angle estimator.

## V. Conclusions

This paper developed an algorithm for estimating Euler angles that describes the attitude between two coordinate systems. The information supplied to the estimator is a sequence of measured components of vectors. Added to the recently published algorithms for estimating the direction cosine matrices (DCM) and the quaternion, this algorithm completes the set of recursive minimum variance algorithms for computing the three common forms of expressing attitude. While the latter was the main objective of this work, it should be remembered that in many cases the vehicle is not an all-attitude vehicle and its steering commands are explicit functions of the Euler angles of the vehicle; thus the use of Euler angles in those cases is advantageous. The choice of parameters to describe the attitude of the vehicle practically dictates the choice of parameters to be used if an estimator is added to the system in order to estimate the attitude from vector measurement. This is so because the estimator needs to compute certain matrices whose entries are readily available if it uses the same parameters that are used in the normal and continuous computation of the attitude from the gyro measurement. This is evident from Eqs. (9) and (27).

While the problem of estimating the DCM and the quaternion from vector measurements involves nonlinear measurements but linear dynamics, the estimation of the Euler angles involves both nonlinear measurements and nonlinear dynamics. The nonlinear equations were linearized and an extended Kalman filter-like algorithm was developed. It was found that if the linearized measurement matrix and the measurement noise covariance matrix were updated before their use in updating the estimation error covariance matrix, the algorithm exhibited better convergence properties and reached steady state in half the time. It was also found that tuning was required to assure convergence when the Euler angles varied in time. Although not designed for all-attitude vehicles, it was found and shown that with the aid of vector measurements, Euler angles can be used for all-attitude vehicles. Monte-Carlo simulation results that demonstrated the effectiveness of the algorithm were presented.

## References

- <sup>1</sup>Shuster, M.D. and Oh, S.D., "Three Axis Attitude Determination from Vector Observations," *Journal of Guidance Control, and Dynamics*, Vol. 4, Jan.-Feb. 1981, pp. 70-77.
- <sup>2</sup>Shuster, M.D., Chitre, D.M., and Niebur, D.P., "In-Flight Estimation of Spacecraft Attitude Sensor Accuracies and Alignment," *Journal of Guidance, Control, and Dynamics*, Vol. 5, July-Aug. 1982, pp. 339-343.
- <sup>3</sup>Lerner G.M., "Three-Axis Attitude Determination," *Spacecraft Attitude Determination and Control*, edited by J.R. Wertz, D. Reidel Publishing Co., Dordrecht, The Netherlands, 1978, pp. 420-428.
- <sup>4</sup>Wahba, G. et al., "Problem 65-1 (Solution)," *SIAM Review*, Vol. 8, 1966, pp. 384-386.
- <sup>5</sup>Brock, J.E., "Optimal Matrices Describing Linear Systems," *AIAA Journal*, Vol. 6, July 1968, pp. 1292-1296.
- <sup>6</sup>Carta, D.G. and Lackowski, D.H., "Estimation of Orthogonal Transformations in Strapdown Inertial Systems," *IEEE Transactions on Automatic Control*, Vol. AC-17, Feb. 1972, pp. 97-100.
- <sup>7</sup>Bar-Itzhack, I.Y. and Reiner, J., "Recursive Attitude Determination from Vector Observations: DCM Identification," *Journal of Guidance, Control, and Dynamics*, Vol. 7, Jan.-Feb. 1984, pp. 51-56.
- <sup>8</sup>Shuster, M.D., "Approximate Algorithms for Fast Optimal Attitude Computation," AIAA Paper 78-1249, Aug. 1978.
- <sup>9</sup>Lefferts, E.J., Markely, F.L., and Shuster, M.D., "Kalman Filtering for Spacecraft Attitude Estimation," *Journal of Guidance, Control, and Dynamics*, Vol. 5, Sept.-Oct. 1982, pp. 417-429.
- <sup>10</sup>Bar-Itzhack, I.Y. and Oshman, J., "Attitude Determination from Vector Observations: Quaternion Estimation," *IEEE Transactions on Aerospace and Electronic Systems*, Vol. AES-21, Jan. 1985, pp. 128-136.
- <sup>11</sup>Gai, E.G., Daly, K.C., Harrison, J.V., and Lemos, L.K., "Star Sensor-Based Satellite Attitude/Attitude Rate Estimator," *Journal of Guidance, Control, and Dynamics*, Vol. 8, Sept.-Oct. 1985, pp. 560-565.
- <sup>12</sup>Kau, S., Kumar, K.S.P., and Granley, G.B., "Attitude Determination Via Nonlinear Filtering," *IEEE Transactions on Aerospace and Electronic Systems*, Vol. AES-5, Nov. 1969, pp. 906-911.
- <sup>13</sup>Farrell, J.L., "Attitude Determination by Kalman Filtering," *Automatica*, Vol. 6, 1970, pp. 419-430.
- <sup>14</sup>Bryson, A.E. and Henrikson, L.J., "Estimation Using Sampled Data Containing Sequentially Correlated Noise," *Journal of Spacecraft and Rockets*, Vol. 5, June 1968, pp. 662-665.
- <sup>15</sup>Gelb, A. (ed.), *Applied Optimal Estimation*, MIT Press, Cambridge, MA, 1974, pp. 293-299.
- <sup>16</sup>Maybeck, P.S., *Stochastic Models, Estimation, and Control*, Vol. 1, Academic Press, New York, 1979, pp. 337-342.

*From the AIAA Progress in Astronautics and Aeronautics Series . . .*

## REMOTE SENSING OF EARTH FROM SPACE: ROLE OF "SMART SENSORS"—v. 67

*Edited by Roger A. Breckenridge, NASA Langley Research Center*

The technology of remote sensing of Earth from orbiting spacecraft has advanced rapidly from the time two decades ago when the first Earth satellites returned simple radio transmissions and simple photographic information to Earth receivers. The advance has been largely the result of greatly improved detection sensitivity, signal discrimination, and response time of the sensors, as well as the introduction of new and diverse sensors for different physical and chemical functions. But the systems for such remote sensing have until now remained essentially unaltered: raw signals are radioed to ground receivers where the electrical quantities are recorded, converted, zero-adjusted, computed, and tabulated by specially designed electronic apparatus and large main-frame computers. The recent emergence of efficient detector arrays, microprocessors, integrated electronics, and specialized computer circuitry has sparked a revolution in sensor system technology, the so-called smart sensor. By incorporating many or all of the processing functions within the sensor device itself, a smart sensor can, with greater versatility, extract much more useful information from the received physical signals than a simple sensor, and it can handle a much larger volume of data. Smart sensor systems are expected to find application for remote data collection not only in spacecraft but in terrestrial systems as well, in order to circumvent the cumbersome methods associated with limited on-site sensing.

*Published in 1979, 505 pp., 6 × 9 illus., \$29.00 Mem., \$55.00 list*

TO ORDER WRITE: Publications Order Dept., AIAA, 1633 Broadway, New York, N.Y. 10019